

THE CLEAVAGE OF SULFONYLUREA HERBICIDE RIMSULFURON[®] UNDER BASIC CONDITIONS: A COMPUTATIONAL INVESTIGATION

Roberta Galeazzi,^{a*} Cesare Marucchini,^b Mario Orena,^{a*} and Gianni Porzi^c

^a Dipartimento di Scienze dei Materiali e della Terra
Università di Ancona – Via Breccie Bianche, I-6031 Ancona, Italy
e-mail: roberta@popcsi.unian.it; orena@popcsi.unian.it

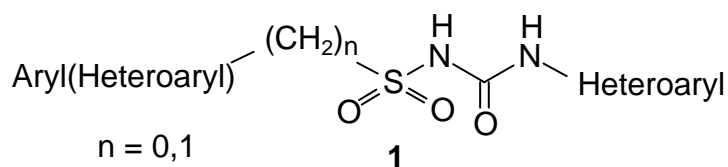
^b Dipartimento Agroambientale e della Produzione Vegetale
Università di Perugia - Borgo XX Giugno 72, I-06121 Perugia, Italy
e-mail: cmaru@unipg.it

^c Dipartimento di Chimica “G. Ciamician
Università di Bologna - Via Selmi 2, I-40126 Bologna, Italy
e-mail: porzi@ciamserv.unibo.it

Abstract - By treatment at pH 9.5, starting from sulfonylurea (**1f**) (Rimsulfuron[®]), the diheteroaryl amine (**3**) is exclusively obtained, whereas under the same conditions sulfonylureas (**1a-e**) showed only cleavage of the SO₂-NH bond. A reaction mechanism proceeding through a five-membered transition state was strongly suggested by both semiempirical and *ab initio* molecular orbital calculations.

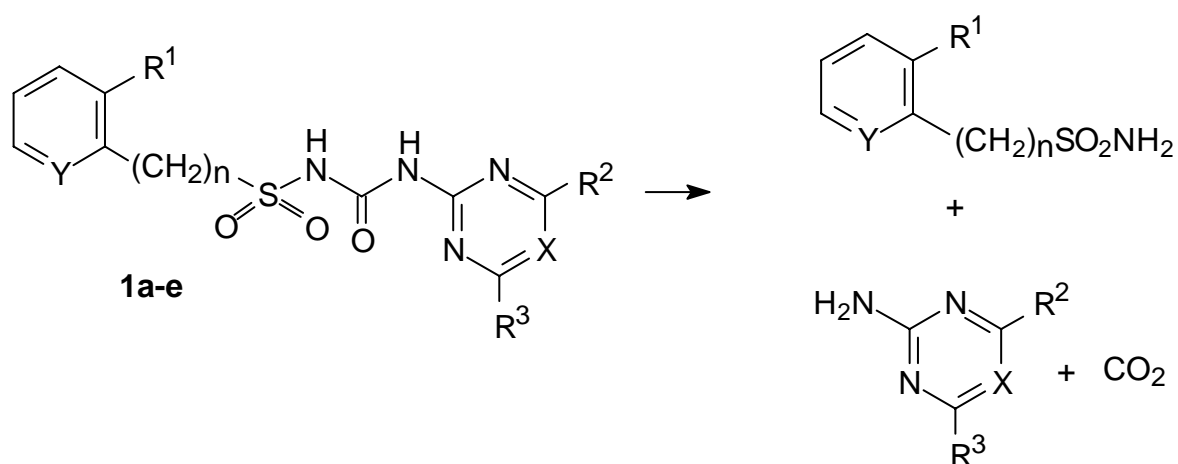
INTRODUCTION

Sulfonylureas (**1**) are inhibitors of acetolactate synthase (ALS), a key enzyme in the biosynthetic pathway of branched-chain amino acids in the plant and are largely employed as weed killers owing to low toxicological effects on mammals. Thus, increased interest arises for their cleavage mechanism occurring in aqueous and soil environment.¹



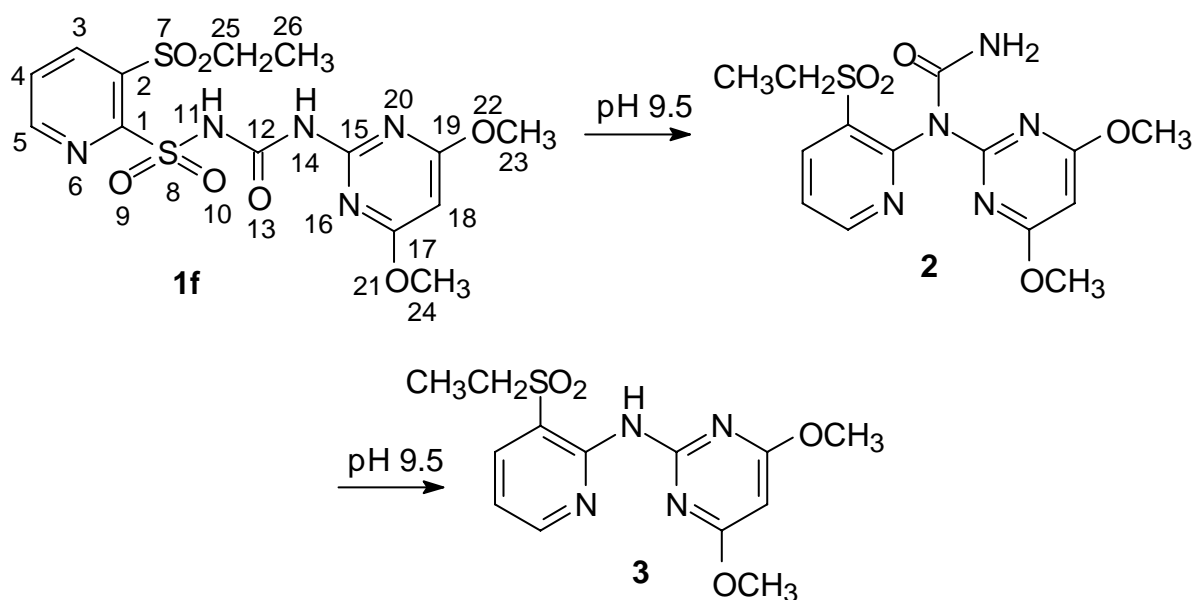
Scheme 1.

Sulfonylureas (**1a-e**) under either acidic (pH 3.5) or basic (pH 9.5) conditions undergo cleavage as reported in Scheme 2.²⁻⁴



Scheme 2. **1a.** Chlorsulfuron[®], X = N, Y = CH, n = 0, R¹ = Cl, R² = CH₃, R³ = OCH₃ **1b.** Sulfometuron methyl[®], X = Y = CH, n = 0, R¹ = COOCH₃, R² = R³ = CH₃ **1c.** Bensulfuron methyl[®], X = Y = CH, n = 1, R¹ = COOCH₃, R² = R³ = OCH₃ **1d.** Primsulfuron[®], X = Y = CH, n = 0, R¹ = COOCH₃, R² = R³ = OCHF₂. **1e.** Prosulfuron[®], X = N, Y = CH, n = 0, R¹ = CH₂CH₂CF₃.

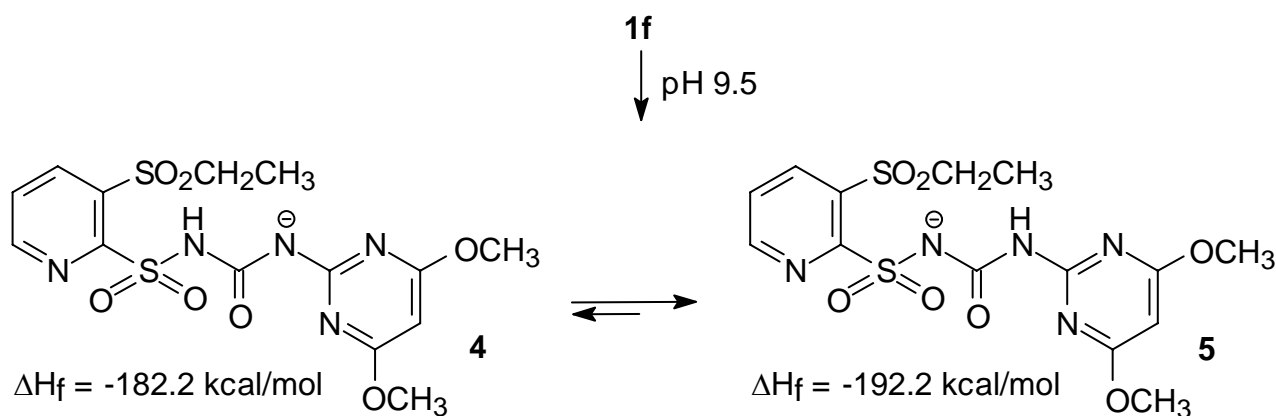
On the contrary, compound (**1f**) (Rimsulfuron[®]) under basic conditions (pH 9.5) is converted into the diheteroarylamine (**3**), exclusively, which could result from contraction of the sulfonylurea bridge through an intramolecular S_NAr reaction (Scheme 3).⁴ With the aim to establish the reaction mechanism, we investigated the behavior of **1f** by using quantumchemical methods (AM1).^{5,6}



Scheme 3.

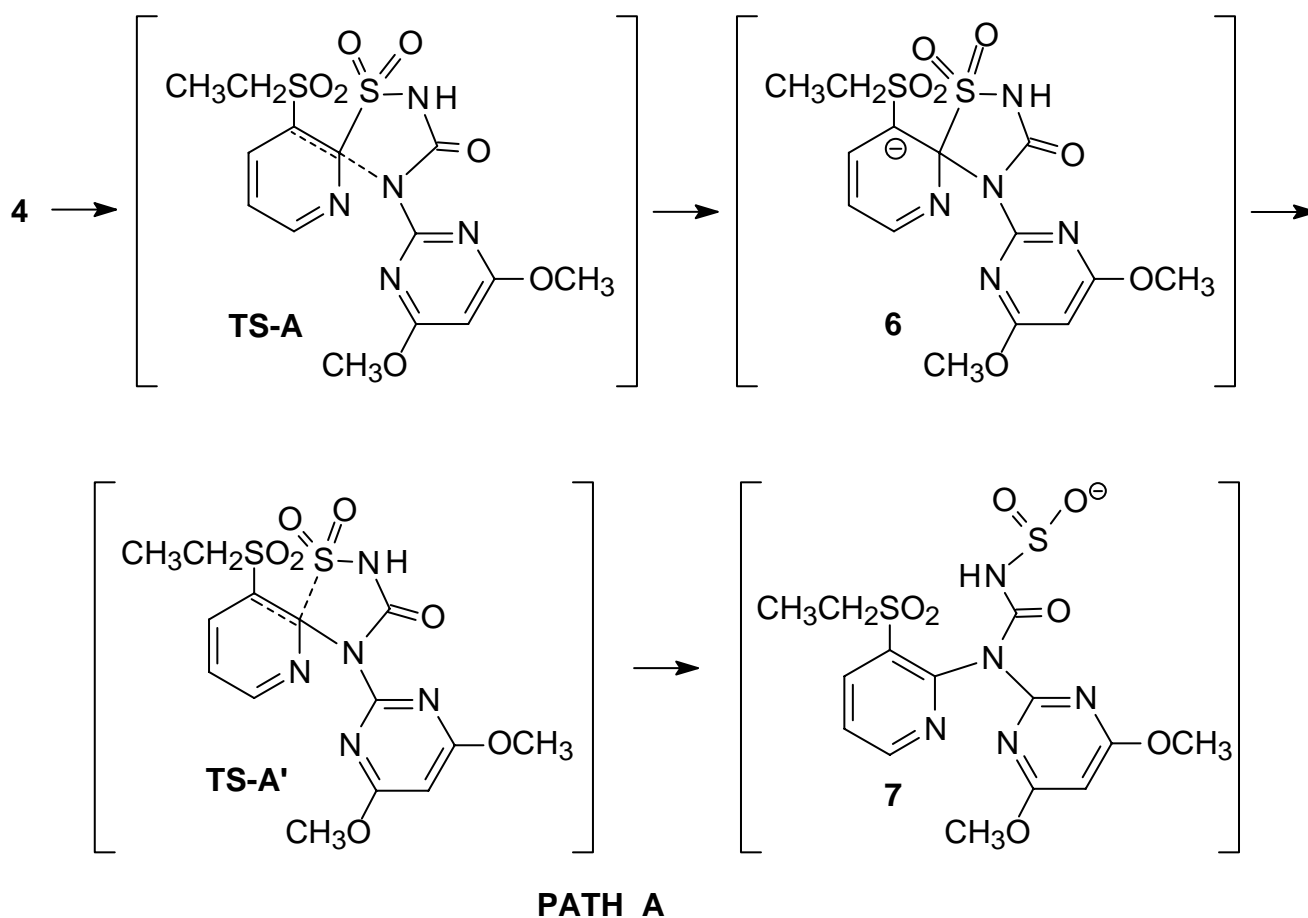
RESULTS AND DISCUSSION

First, the geometries of anions (**4**) and (**5**), which arise from **1f** at pH 9.5, were calculated together with the corresponding minimum energy conformations (Scheme 4). Thus, at pH 9.5 the anion (**5**) resulted to be the major component of the equilibrium mixture, being more stable than **4** by 10 kcal/mol (Scheme 4).¹



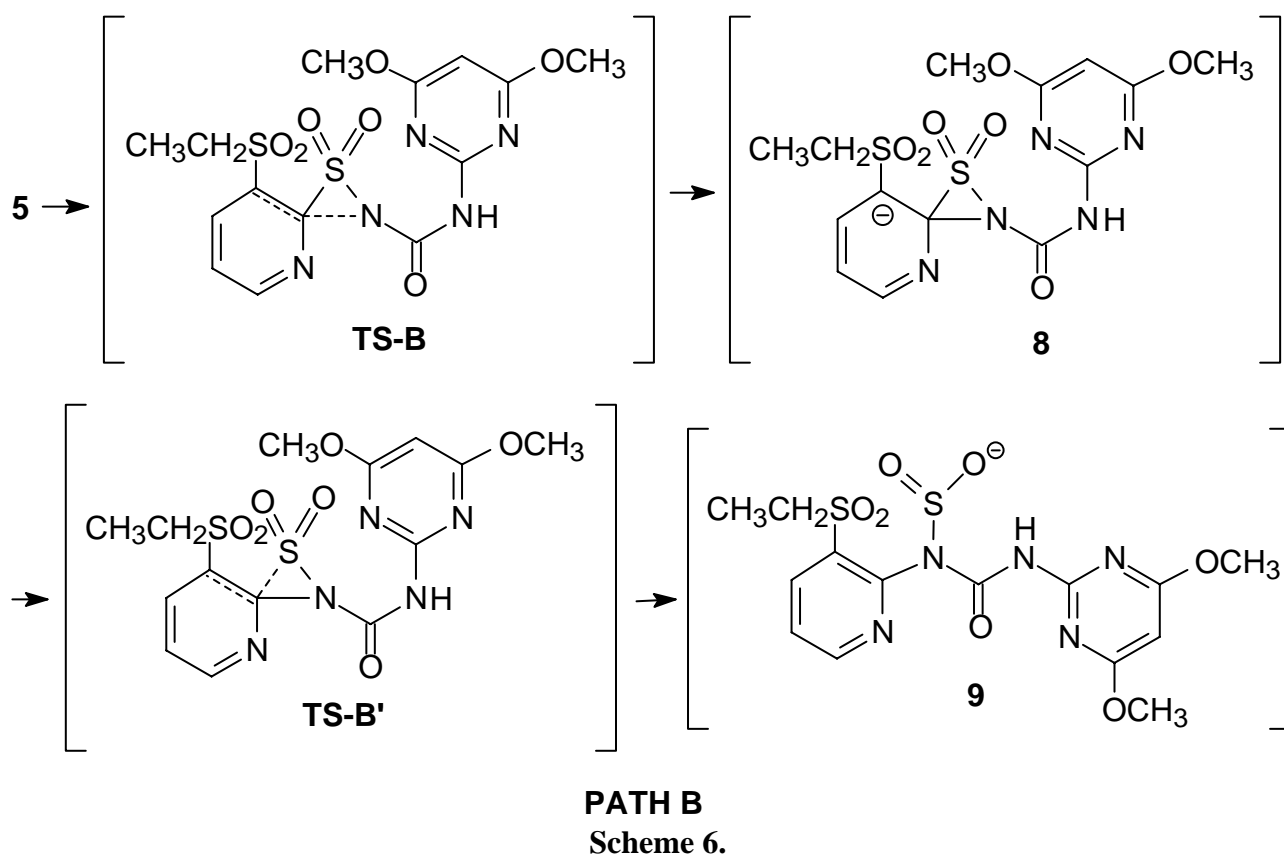
Scheme 4.

Although the product (**3**) verosimilarly arises from anion (**4**) through a five-membered transition state, we examined also the cleavage mechanism proceeding through a three-membered transition state, starting from the anion (**5**) which is predominant at pH 9.5, in order to reject this pathway already reported for intramolecular S_NAr .⁷ Thus, two reaction paths were taken in account, path **A**, proceeding through a five-membered transition state, and path **B**, proceeding through a three-membered one. In fact, starting from anion (**4**), the intermediate (**6**) having a moderate angular strain is formed through the five-membered transition state **A** (Pathway **A**), to give subsequently **7** through transition state **A'** (Scheme 5).



Scheme 5.

On the contrary, attack of the anion (**5**) at C-2 of the pyridine ring through transition state **B** (Pathway B), leading to the three-membered intermediate (**8**), occurs with high angular strain to give eventually product (**9**) through transition state **B'** (Scheme 6).



In order to definitely establish the reaction mechanism, for each pathway we located two transition states (**A** and **A'** for path A and **B** and **B'** for path B) and two intermediates (**6** and **7** in the former case and **8** and **9** in the latter), as reported in Figure 1.

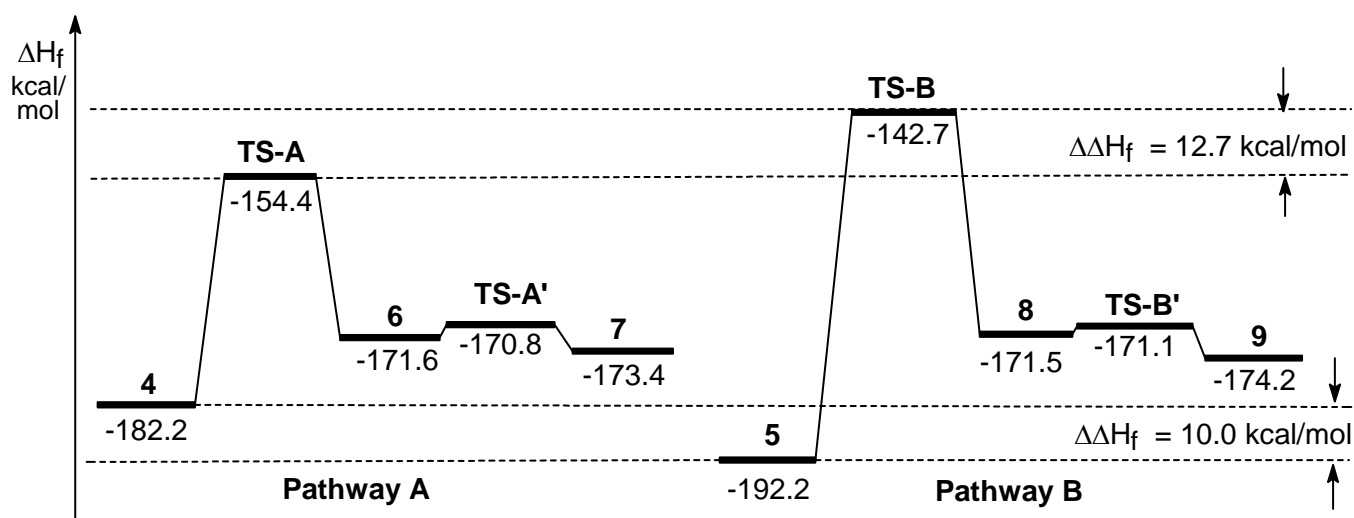
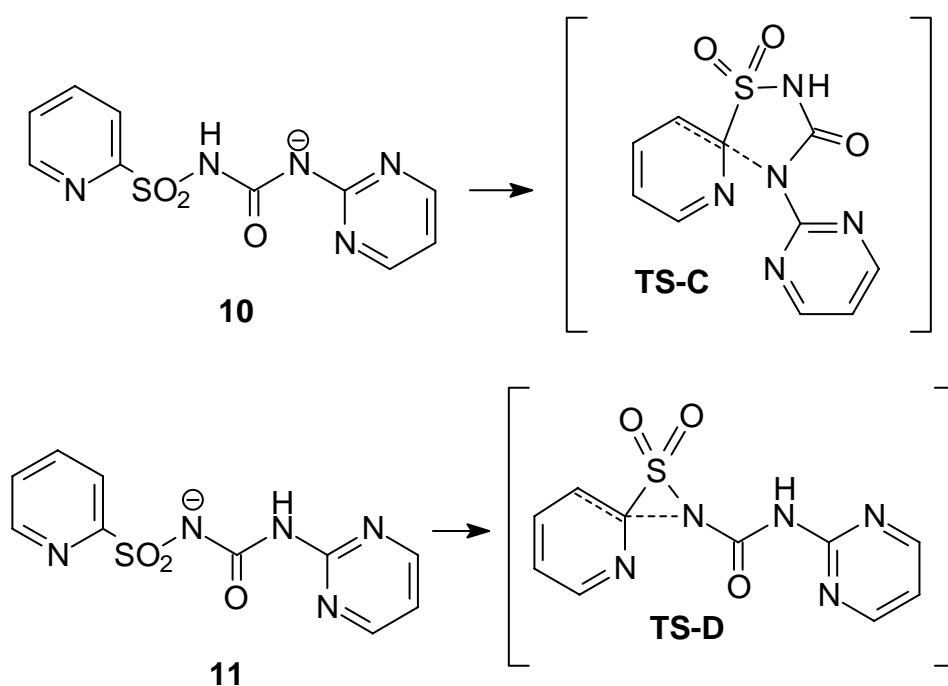


Figure 1. Energy profiles for pathways A and B.

The ΔH^\ddagger values of both transition states **A'** and **B'** are very small and similar, whereas ΔH^\ddagger values for transition states **A** and **B** resulted to be 27.8 and 49.5 kcal/mol respectively. As a consequence, path A is largely preferred over path B owing to the large difference of ΔH^\ddagger between the rate determining steps. In order to test the reliability of the AM1 Hamiltonian in describing these molecular systems, we investigated the modeling of the reaction by means of *ab initio* methods. Since the complete theoretical study of the possible reaction pathways is heavy and difficult due to the computational effort, the first step of the reaction was exclusively considered and calculations were performed on simpler model structures (**10**) and (**11**), leading to transition states **C** and **D**, respectively (Scheme 7).



Scheme 7.

The structures of both reactants and transition states were located and optimized at both RHF/3-21G* and RHF/6-31G* level,¹⁰ and then single point calculations were carried out at B3LYP/6-31G* level to take the electronic correlation into account, and results are reported in Tables 1 and 2. It is worth noting that a good agreement between semiempirical and *ab initio* molecular orbital calculation results even from the lower level *ab initio* calculations.¹¹

Table 1. Calculated energies of the reactants and transition structures for the model reaction at semiempirical (AM1, kcal/mol) and *ab initio* (B3LYP/6-31G*//RHF/3-21G*, atomic units) theory levels.

Structure	AM1	B3LYP/6-31G* //RHF/3-21G*
10	-40.7	-1283.47624
TS-C	-3.3	-1283.43453
11	-49.4	-1283.47635
TS-D	4.9	-1283.41006

Table 2. Calculated energies of the reactants and transition structures for the model reactions at semiempirical (AM1, kcal/mol) and *ab initio* (B3LYP/6-31G**/RHF/6-31G*, atomic units) theory levels.

Structure	AM1	B3LYP/6-31G* //RHF/6-31G*
10	-40.7	-1283.47808
TS-C	-3.3	-1283.43453
11	-49.4	-1283.47865
TS-D	4.9	-1283.41006

For the purpose of comparison, the same structures were located at the semiempirical level AM1. The calculated geometries of optimised structures are displayed in Figures 2 and 3, together with relevant atomic distances and bond angles.

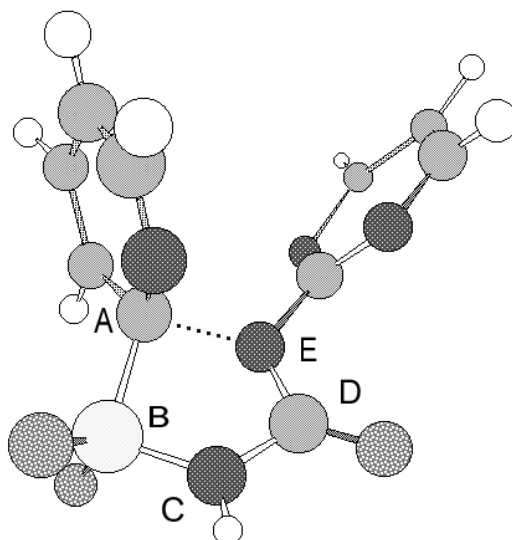


Figure 2. Calculated *ab initio* RHF/6-31G* and AM1 (italic) geometries for transition state **C** [AB = 1.7598 (*1.8160*) Å, BC = 1.6232 (*1.6258*) Å, CD = 1.4032 (*1.4249*) Å, DE = 1.3576 (*1.4059*) Å, EA = 1.7052 (*1.7630*) Å. ABC = 95.51° (*97.93*°), BCD = 116.35° (*116.37*°), CDE = 107.08° (*110.75*°)].

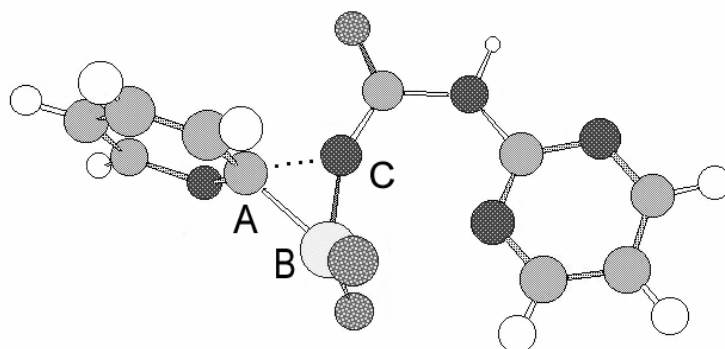


Figure 3. Calculated *ab initio* RHF/6-31G* and AM1 (italic) geometries for transition state **D** [AB = 1.8875 (*1.8335*) Å, BC = 1.6404 (*1.6037*) Å, CA = 1.6001 (*1.5670*) Å, ABC = 53.39° (*53.77*°)].

Table 3. Activation energy E_a (kcal/mol) for reaction paths A and B.

Path	AM1	B3LYP/6-31G*// RHF/3-21G*	B3LYP/6-31G*// RHF/6-31G*
10-TS-C	37.4	26.2	27.3
11-TS-D	54.3	41.6	43.0

It is worth noting that both the AM1 and *ab initio* calculations predicts the same results, as it appears from Tables 1-3. As a consequence, since in each case the most stable transition state resulted to be the same, irrespective of the level theory used, comparison between semiempirical and *ab initio* results can be extrapolated to the reaction studied.

With the aim to get a deeper insight into the reaction mechanism, we eventually studied interactions between the LUMO and the HOMO of both anions (**4**) and (**5**) by means of AM1 Hamiltonian. Thus, MO calculations were carried out, in order to obtain shapes and orientations of the frontier orbitals HOMO and LUMO and subsequently the frontier electron densities were calculated in order to characterise the donor-acceptor interaction.¹⁴ For **4**, it resulted that both HOMO and LUMO have the highest contribution for N-14 and C-1, respectively, which must be involved in the S_NAr process. In addition, these orbitals have also the proper orientation allowing the correct superimposition during S_NAr reaction (Table 4). On the contrary, for anion (**5**), the HOMO has no contribution from N-11, while N-14 is still an important donor site and LUMO has a significant, although smaller contribution arising from C-1. Moreover, since in **5** the HOMO contribution at N-11 is practically missing, whereas it is significant at N-14, it results that S_NAr must involve C-1 and N-14, exclusively. In addition, for **4** the highest f_r^N for LUMO lies at C-1 (acceptor site), and f_r^E for HOMO at N-14 (donor site), respectively (Table 4), whereas for anion (**5**) the highest f_r^N for LUMO lies at C-5, and f_r^E for HOMO lies at C-18 (Table 4), in agreement with the proposed mechanism.

Table 4. Significant frontier electron density values for anion (**4**).

Atom	f_r^E HOMO	Atom	f_r^N LUMO
N-14	0.329	C-1	0.250
N-16	0.128	C-2	0.245
C-18	0.300	C-4	0.132
N-20	0.124	C-5	0.207
N-11	0.007		

Table 5. Significant frontier electron density values for anion (**5**).

Atom	f_r^E HOMO	Atom	f_r^N LUMO
N-14	0.267	C-1	0.150
N-16	0.104	C-2	0.254
C-18	0.361	C-4	0.098
N-20	0.105	C-5	0.301
N-11	0.015		

CONCLUSION

In conclusion, both AM1 and *ab initio* calculations supported that a five-membered transition state is involved in the cleavage of sulfonylurea (**1f**) (Rimsulfuron[®]) at pH 9.5. Moreover, since the results obtained from both AM1 and *ab initio* calculations are in good agreement, AM1 could be employed to study these molecular systems.

THEORETICAL CALCULATIONS

All simulations were carried out in gas-phase using the AM1 quantum mechanical method as implemented in HyperChem 5.1 (PC version) and 4.5 (SGI version) molecular modeling packages.^{6,7} The conformational search¹⁵ was performed by using a MonteCarlo algorithm¹⁵ included in the package varying all internal degree of freedom, and all the conformers having energy within 3 Kcal/mol were considered. All the calculations were performed on both Silicon Graphics Indigo2 workstation R10000 175 MHz and SGI O2 R10000 195 MHz and on a PC Pentium MMX 266 MHz.

The synchronous transit method was chosen to localize the transition states,¹⁵ at the AM1 Hamiltonian level as implemented in HyperChem 5.1 Software Package, and we used the quadratic synchronous transit (QST) implementation.^{16,17} In order to complete the calculation and find well refined structure, an eigenvector-following step was used.¹⁸ An extensive characterisation of the potential energy surface was performed in order to ensure that optimized structures were true transition states. These stationary points were characterized by performing a vibrational analysis and the Hessian matrix was calculated. It resulted that these **TS** structures were all first order saddle points on the potential energy surface (PES) since they have only one imaginary frequency corresponding to the right coordinate of reaction, i.e. to the formation of the new N-C bond. In fact it consists in a synchronous motion of the two centres of reaction involved.¹⁹ *Ab initio* calculations were carried out using Gaussian-94 program.⁹ Full geometry optimizations were performed at the RHF/3-21G* and RHF/6-31G* level for all the minima and transition structures using the Berny algorithm. On all these structures a complete vibrational analysis was performed with the aim to check the nature of these stationary points. The TS have only one imaginary frequency corresponding to the expected c.d.r.²⁰ Single point RHF/3-21G* MP2, calculations¹⁰ were carried out using the geometries optimized at the RHF/3-21G* level, whereas single point B3LYP/6-31G* calculations were carried out using the geometries optimized at both the RHF/3-21G* and RHF/6-31G* level.¹¹

The heats of formation and the quantum chemical descriptors (HOMO and LUMO distribution and frontier electron density) were also obtained at AM1 level. The m.o. calculations were carried out on the lowest energy conformation of the examined compounds. Frontier orbital electron densities were calculated on the basis of the atomic orbitals coefficients of HOMO and LUMO respectively. In the case of a donor molecule, the HOMO density is critical to the charge transfer (electrophilic electron density f_r^E) and in the case of an acceptor molecule the LUMO density is important (nucleophilic electron density f_r^N).²¹

ACKNOWLEDGEMENT

This research was supported by C.N.R., (Rome) and partially by M.U.R.S.T. (Italy) within the project "Pesticide Fate in the Soil-Plant System".

REFERENCES AND NOTES

1. G. Levitt, in *Pesticide Chemistry: Human Welfare and Environment*, ed. by J. Miyamoto and P. C. Kearney, 1983, Vol. 1, Pergamon Press, New York, p. 243; R. F. Sauers and G. Levitt, in *Pesticide Synthesis through Rational Approaches*, ed. by P. S. Magee, G. K. Kohn and J. J. Mean, 1984, American Chemical Society, Washington, p. 21; E. M. Beyer, M. J. Duffy, J. V. Hay and D. D. Schlueter, *Sulphonylurea Herbicides in Herbicides: Chemistry, Degradation and Mode of Action*, ed. by P. C. Kearney and D. D. Kaufman, 1988, Vol. 3, Marcel Dekker, New York, pp. 117-189; B. M. Berger, N.L. Wolfe, *Environm. Toxicol. & Chem.*, **1996**, *15*, 1500.
2. L. M. Shalaby, F. Q. Bramble, Jr. and P. W. Lee, *J. Agric. Food Chem.*, **1992**, *40*, 513.
3. H. J. Streck, *Pestic. Sci.*, **1998**, *53*, 29. L. D. Bray, N. E. Heard, M. C. Overman, J. D. Vargo, D. L. King, L. J. Lawrence and A. W. Phelps, *Pestic. Sci.*, **1997**, *51*, 56.
4. G. E. Schneiders, M. K. Koeppel, M. V. Naidu, P. Horne, A. M. Brown and C. F. Mucha, *J. Agric. Food Chem.*, **1993**, *41*, 2404; C. Marucchini and R. Luigetti, *Pestic. Sci.*, **1997**, *50*, 102.
5. M. J. S. Dewar, E. G. Zoebisch, E. F. Healy and J. J. P. Stewart, *J. Am. Chem. Soc.*, **1985**, *107*, 3902; M. J. S. Dewar and K. M. Dieter, *J. Am. Chem. Soc.*, **1986**, *108*, 8075; J. J. P. Stewart, *J. Comp. Aid. Mol. Design*, **1990**, *4*, 1; J. J. P. Stewart, *J. Comput. Chem.*, **1989**, *10*, 209; J. J. P. Stewart, *ibid.*, **1989**, *10*, 221.
6. Hyperchem releases 4.5 and 5.1 and Chemplus release 1.6, from Hypercube, Inc., Gainesville, Florida, U.S.A.
7. T. Fukuyama, M. Cheung, C.-K. Jow, Y. Hidai and T. Kan, *Tetrahedron Lett.*, **1997**, *38*, 5831.
8. The frequency values are the following: for transition state **A**, 565.53i cm⁻¹; for transition state **A'**, 354.34i cm⁻¹; for transition state **B**, -20.1i cm⁻¹; for transition state **B'**, -50.65i cm⁻¹.
9. M. J. Frish, G. W. Trucks, H. B. Schlegel, P. M. W. Gill, B. G. Johnson, M. A. Robb, J. R. Cheeseman, T. A. Keith, G. A. Petersson, J. A. Montgomery, K. Raghavachari, M. A. Al-Laham, V. G. Zakrzewski, J. V. Ortiz, J. B. Foresman, J. Cioslowski, B. B. Stefanov, A. Nanayakkara, M. Challacombe, C. Y. Peng, P. Y. Ayala, W. Chen, M. W. Wong, J. L. Andres, E. S. Replogle, R. Gomperts, R. L. Martin, D. J. Fox, J. S. Binkley, D. J. Defrees, J. Baker, J. P. Stewart, M. Head-Gordon, C. Gonzalez and J. A. Pople, *Gaussian 94*, Gaussian, Inc., Pittsburg, PA, 1995.
10. C. C. Roothan, *Rev. Mod. Phys.*, **1951**, *23*, 69; M. Head-Gordon, J. A. Pople and M. J. Frish, *Chem. Phys. Lett.*, **1988**, *153*, 503. S. Saebo and J. Almlöf, *Chem. Phys. Lett.*, **1989**, *154*, 83.
11. C. Lee, W. Yang and R. G. Parr, *Phys. Rev. B*, **1988**, *37*, 785; A. D. Becke, *Phys. Rev. A*, **1988**, *38*, 3098; B. Mihelich, A. Savin, H. Stoll and H. Preuss, *Chem. Phys. Lett.*, **1989**, *157*, 200; A. D. Becke, *J. Chem. Phys.*, **1993**, *98*, 5648.
12. H. B. Schlegel, *J. Comp. Chem.*, **1982**, *3*, 214; R. Fletcher and M. J. D. Powell, *Comput. J.*, 1963, *6*, 163; B. A. Murtaugh and R. W. H. Sargent, *Comput. J.*, **1970**, *13*, 185; J. Baker, *J. Comp. Chem.*, **1986**, *7*, 385; J. Baker, *J. Comp. Chem.*, **1987**, *8*, 563; H. B. Schlegel, in *New Theoretical Concepts for Understanding Organic Reactions*, ed. by J. Bertran, Kluwer Academic, The Netherlands, 1989, pp. 33-53.
13. R. Franke, *Theoretical Drug Design Methods*. 1989, Elsevier, Amsterdam, p. 115; K. Fukui, *Theory of Orientation and Stereoselection*, 1975, p. 34, Springer Verlag, New York; I. Fleming, *Frontier Orbitals and Organic Chemical Reactions*, 1976, J. Wiley & Sons, London.
14. Y. S. Pabthakar, *Drug Des. Delivery*, **1991**, *7*, 227; M. Karelson, V. S. Lobanov and A. R. Katritzky, *Chem. Rev.*, **1996**, *96*, 1027.
15. A. R. Leach, *A Survey of Methods for Searching the Conformational Space of Small and Medium Sized Molecules*, in *Reviews in Computational Chemistry*, ed. by K. B. Lipkowitz and D. B. Boyd, 1991, VCH Publishers, Inc., New York, pp. 1-56; C. E. Peishoff and J. S. Dixon, *J. Comput. Chem.*,

- 1992**, *13*, 565; H. Goto and E. Osawa, *J. Chem. Soc., Perkin Trans. 2*, **1993**, 187; H. Goto and E. Osawa, *J. Am. Chem. Soc.*, **1989**, *111*, 8950; I. Kolossváry and W. C. Guida, *J. Comput. Chem.*, **1993**, *14*, 691; B. Von Freyberg and W. Braun, *J. Comput. Chem.*, **1991**, *12*, 1065; M. Saunders, K. N. Houk, Y.-D. Wu, W. C. Still, M. Lipton, G. Chang and W. C. Guida, *J. Am. Chem. Soc.*, **1990**, *112*, 1419.
16. G. Chang, W. C. Guida and W. C. Still, *J. Am. Chem. Soc.*, **1989**, *111*, 4379; J. M. Goodman and W. C. Still, *J. Comput. Chem.*, **1991**, *12*, 1110.
17. A. Banerjee, N. Adams, J. Simons and R. Shepard, *J. Phys. Chem.*, **1985**, *89*, 52; J. Simons and J. Nichols, *Int. J. Quant. Chem., Quantum Chem. Symp.*, 1990, *24*, 263.
18. C. Peng and H.B. Schlegel, *Isr. J. Chem.*, **1993**, *33*, 449.
19. J. Baker, *J. Comput. Chem.*, **1986**, *7*, 385.
20. The frequency values are the following: 239.31i cm⁻¹ (3-21G*) and 353.77i cm⁻¹ (6-31G*) for transition state **C**; 401.06i cm⁻¹ (3-21G*) and 459.82i cm⁻¹ (6-31G*) for transition state **D**.
21. To compare the reactivities of different molecules, frontier electron densities can be normalized by the energy of corresponding frontier molecular orbitals (F_r^E (HOMO) and F_r^N (LUMO)): R. Franke, *Theoretical Drug Design Methods*, Elsevier, Amsterdam, 1984, pp. 115-123; A. Nakayama, K. Hagiwara, S. Hashimoto and S. Shimoda, *Quant. Struct.-Act. Relat.*, **1993**, *12*, 251.